PERGAMON

Journal of Structural Geology 24 (2002) 1669–1675

JOURNAL OF STRUCTURAL GEOLOGY

www.elsevier.com/locate/jstrugeo

An alternative model for the growth of faults

J.J. Walsh[a,*], A. Nicol[b], C. Childs[a]

[a]*Fault Analysis Group, Department of Geology, University College Dublin, Belfield, Dublin 4, Ireland*
[b]*Institute of Geological and Nuclear Sciences, PO Box 30368, Lower Hutt, New Zealand*

Received 16 January 2001; revised 7 July 2001; accepted 27 November 2001

Abstract

Conventional growth models suggest that faults become larger due to systematic increases in both maximum displacement and length. We propose an alternative growth model where fault lengths are near-constant from an early stage and growth is achieved mainly by increase in cumulative displacement. The model reconciles the scaling properties of faults and earthquakes and predicts a progressive increase in fault displacement to length ratios as a fault system matures. This growth scheme is directly applicable to reactivated fault systems in which fault lengths were inherited from underlying structure and established rapidly; the model may also apply to some non-reactivated fault systems. Near-constant fault lengths during subsequent growth are attributed to retardation of lateral propagation by interaction between fault tips. The model is validated using kinematic constraints from growth strata, which are displaced by a system of reactivated normal faults in the Timor Sea, NW Australia. © 2002 Elsevier Science Ltd. All rights reserved.

Keywords: Fault displacement; Fault length; Fault growth; Earthquakes

1. Introduction

Quantitative constraints from ancient fault systems indicate that maximum displacement (D) scales with fault-trace length (L), following the expression:

$$D = cL^n,$$

where c is a constant and n is between 1 and 1.5 (e.g. Walsh and Watterson, 1988; Cowie and Scholz, 1992; Gillespie et al., 1992; Dawers et al., 1993; Schlische et al., 1996). Irrespective of the precise value of n, the conventional explanation for this relationship is that it represents a growth trend with faults becoming larger due to systematic increases in both maximum displacement and length (Fig. 1). This growth model has not, however, been tested using kinematic constraints on faults and questions remain regarding its general applicability.

Fault growth is generally attributed to the superimposition of many earthquake slip events on a fault surface, and a growth model for faulting must demonstrate a link between the scaling properties of faults and earthquakes. Historical earthquakes indicate that slip scales linearly with fault-rupture length (e.g. Scholz, 1982; Wells and Coppersmith, 1994). The slip to length ratio of earthquakes is therefore approximately constant (ca. 5×10^{-5} from Wells and Coppersmith, 1994), and only large faults can accommodate large-magnitude earthquakes. Large faults may also rupture during earthquakes of small or moderate size (e.g. Cowie and Shipton, 1998), however, earthquake-scaling properties, such as the Gutenberg–Richter relationship, demonstrate that large earthquakes contribute disproportionately more to the strain accommodated within a fault system or along a fault (Scholz and Cowie, 1990).

Established fault-growth models predict that the earliest formed faults had lengths that were significantly shorter than their final lengths (Walsh and Watterson, 1988; Cowie and Scholz, 1992). The first earthquake generated for each of these early faults would have had a slip to length ratio described by the earthquake-scaling relationship (e.g. Scholz, 1982; Wells and Coppersmith, 1994). Comparison of fault and earthquake populations suggests, however, that faults have much higher displacement to length ratios than individual earthquakes, a feature which is at odds with the belief that fault-growth trends define lines of constant displacement to length ratio. This problem is less acute for growth models in which $n = 1.5$, because fault-growth curves intersect the earthquake-scaling relationship at short fault lengths and can also generate the high displacement to length ratios that are typical of faults.

Here we present an alternative growth model for faults that is consistent with the existing displacement–dimension data and provides a link between earthquake and fault

* Corresponding author. Tel.: +353-1-7062606; fax: +353-1-7062607.
E-mail address: john@fag.ucd.ie (J.J. Walsh).

0191-8141/02/$ - see front matter © 2002 Elsevier Science Ltd. All rights reserved.
PII: S0191-8141(01)00165-1

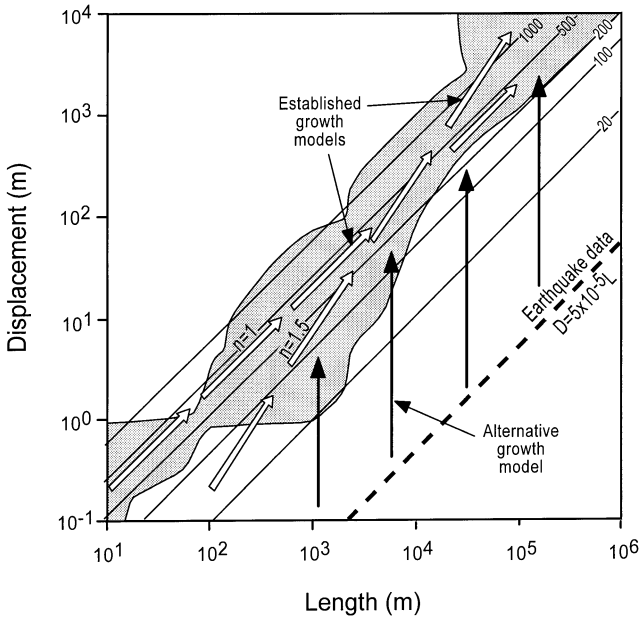

Fig. 1. Log–log plot of maximum displacement vs. length showing growth paths of faults for the established models and our alternative model. Shaded area outlines the field of existing data (Schlische et al., 1996; $n = 547$), while the average position of earthquake data for all types of faults from Wells and Coppersmith (1994) is indicated by the thick dashed line. Contours of 20, 100, 200, 500 and 1000 indicate the number of earthquakes (N) required to move cumulative fault displacements along vertical growth trends from the earthquake line. Contours were determined for displacement per earthquake of $D_{\text{earthquake}} = (5 \times 10^{-5})L_{\text{earthquake}}$ (Wells and Coppersmith, 1994) where $L_{\text{earthquake}}$ (earthquake rupture length) is constant for a given fault and equal to the total fault length and $N = D_{\text{total}}/D_{\text{earthquake}}$.

observations. In this new growth model, fault lengths are established rapidly and subsequent interaction between faults retards lateral propagation producing essentially constant lengths for much of the duration of faulting. As a consequence of minimal lateral propagation, growth paths for faults on a displacement–length plot are near-vertical and oblique to the established trend of the data; the established trend cannot therefore be regarded as a growth trend (Fig. 1). In support of the model we present growth curves for a system of reactivated normal faults in the Timor Sea, where faults maintained near-constant fault lengths as displacement accumulated, and the final displacements and lengths lie within the established trend.

2. Alternative growth model

The initial size distribution of faults at the earliest stages of fault development is unknown. Previous models predict that faults initially have short lengths, which fall within a narrow range of sizes (e.g. Walsh and Watterson, 1988; Cowie and Scholz, 1992; Gillespie et al., 1992). If, however, the lengths of faults at an early stage cover a much broader range of fault sizes, then the early displacement (i.e. the slip arising from one or a small number of earthquakes), will be

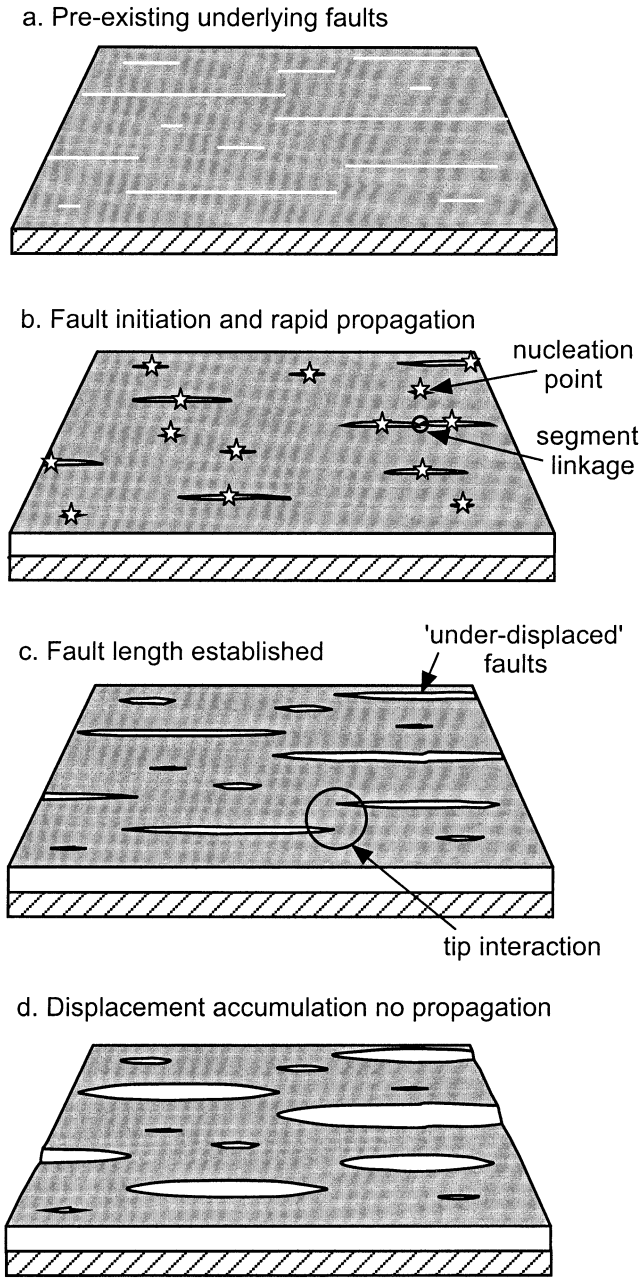

Fig. 2. Schematic block diagram illustrating our alternative fault growth model using sequential fault maps from the base of a syn-faulting sequence (b–d). (a) Shows the locations of pre-existing faults in the rocks beneath the faulted horizon. (b) Faulting initiates on the horizon above the pre-existing fault system with nucleation close to the centre of each fault. Fault lengths increase rapidly while displacements accrue relatively slowly. (c) Propagation ceases when the faults begin to interact, while displacement continues to accumulate at near constant rates. Fault lengths are inherited from a pre-existing fault system (a). (d) Fault lengths remain fixed while displacements accrue.

significantly lower than that expected from established displacement–length relationships, producing faults that are ‘under-displaced’ for their lengths (Fig. 2). This may appear to contravene the basic scaling properties of faults, though a plausible growth model can be constructed, which

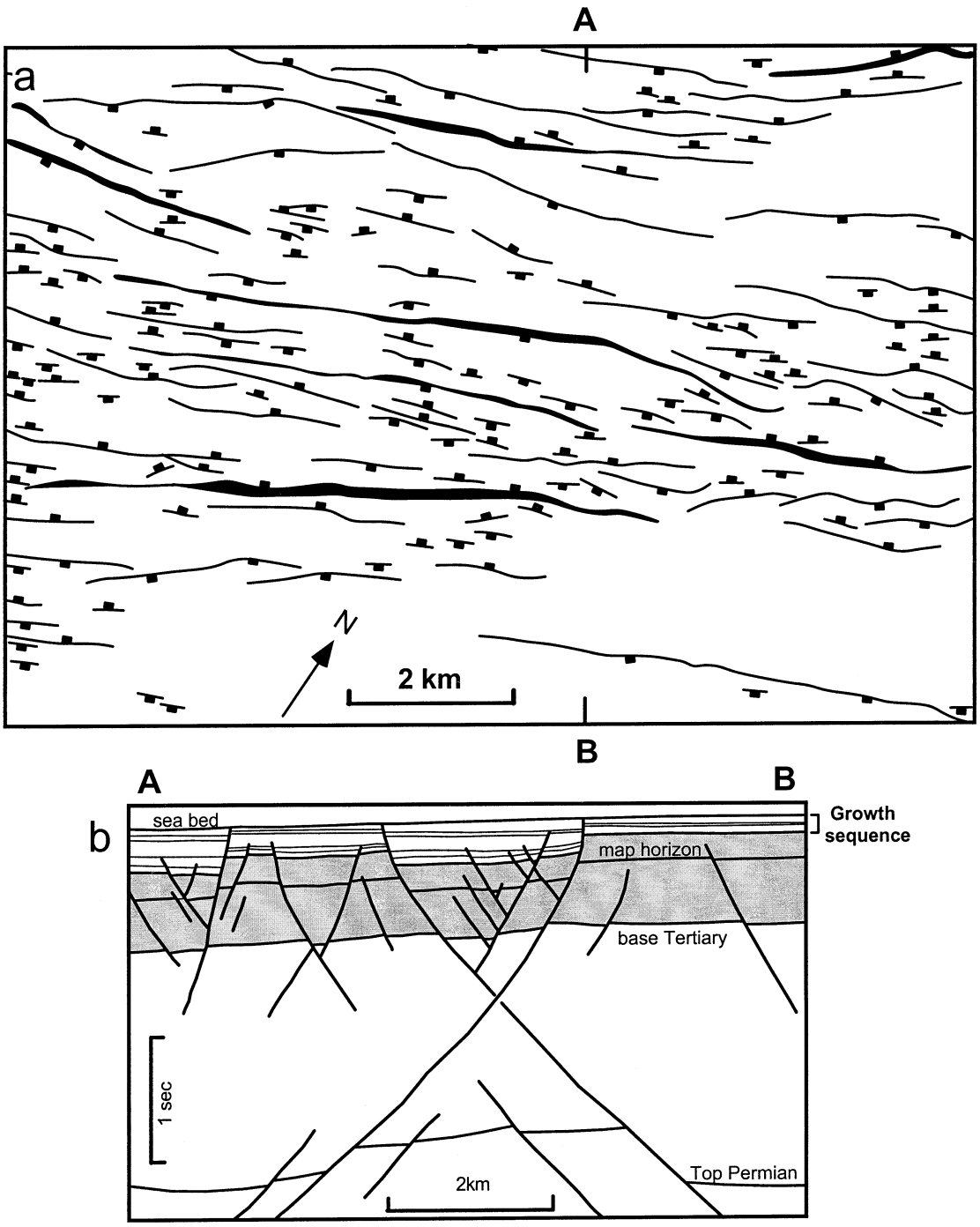

Fig. 3. (a) Map of normal faults in the Timor Sea, which offset the base of the syn-faulting sequence (modified from Meyer et al. (2002)). Fault-trace widths are proportional to displacement on the map horizon. (b) Cross-section approximately normal to the strike of faults showing the syn-faulting sequence (i.e. growth sequence) and map horizon in (a). The vertical scale is in two-way travel time and the cross-section is approximately at true scale within the Tertiary sequence. For an example of the seismic data see Meyer et al. (2002).

reconciles these displacement–dimension relations at an early stage of faulting with data from mature fault systems.

Given a broad range of fault lengths from the early stages of deformation, the size of earthquakes on 'under-displaced' faults will also vary from the early stages. Displacement on these faults is sufficiently 'under-displaced' that fault propagation is minimal and faults grow principally by increases in displacement. These displacement increases are achieved by the superimposition of earthquakes, the largest and most important of which rupture the entire fault surface and scale with fault length. For this model fault-growth curves

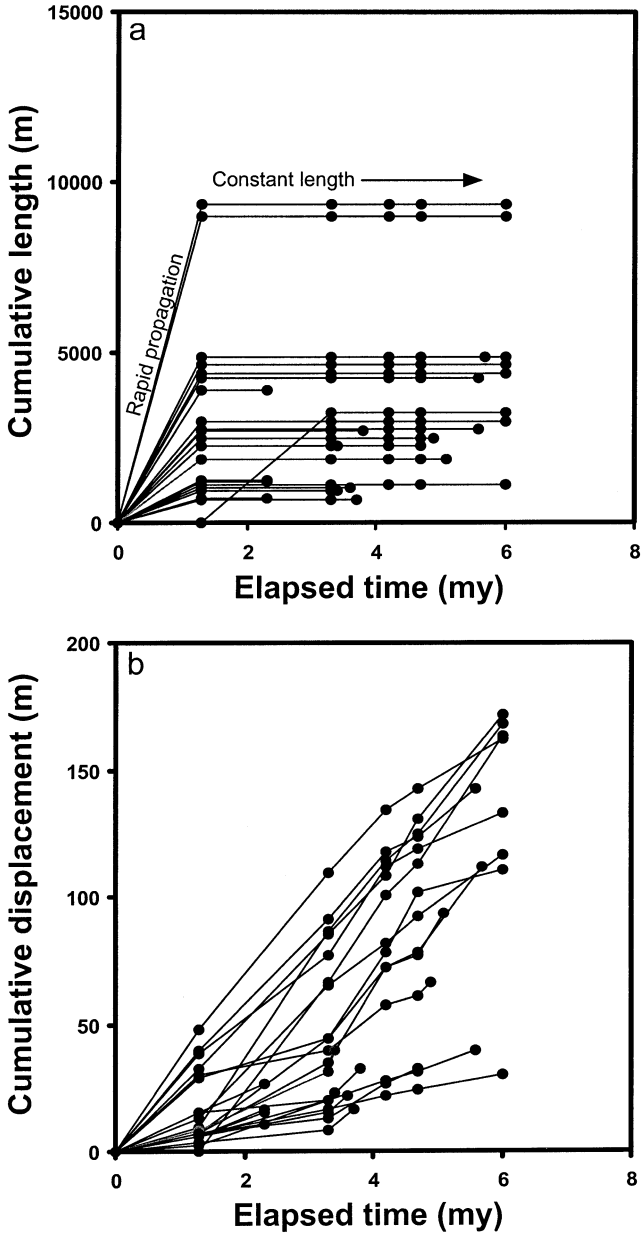

Fig. 4. Growth curves for 23 of the largest faults from the Timor Sea dataset showing changes in fault length (a) and maximum displacement (b) with increase in elapsed time from the onset of extension. Faults that became inactive during extension have maximum values of elapsed time <6 my.

are steep and the scaling trends for faults show a progressive increase in displacement to length ratio with time (Fig. 1). In cases where all faults continue to grow, trends with constant displacement to length ratios for the entire population of faults only require that earthquake slip scales with fault length (Scholz 1982; Wells and Coppersmith 1994) and that the repeat times of earthquakes do not vary significantly with fault length.

Whether the predictions of the model violate the established scaling properties of real fault systems depends, to a great extent, on how rapidly the fault-scaling trends converge on those established from previous studies. Fig. 1 shows that in 20 to 200 earthquakes, fault displacement to length ratios begin to overlap with previously measured data. For a range of average repeat times of ca. 100 to 10,000 years for earthquakes, this model suggests that the scaling properties of faults begin to fall within accepted ranges after 2000 to 2,000,000 years of faulting. On geological time scales, these periods are either effectively instantaneous or short compared with the longevity of typical fault systems. For example, time intervals of up to 2,000,000 years comprise ≤30% of the entire 6 my period of faulting in the Timor Sea data set (see Section 3) and ≤8% of the 25 my syn-rift interval in parts of the North Sea (McLeod et al., 2000). The model is therefore capable of rapidly generating the established trends of fault data for most fault systems, but following growth trends that are at variance with established models. 'Under-displaced' faults may, therefore, occur in regions of minor extension (e.g. <0.5%). In these circumstances, however, sedimentary basins are unlikely to have formed in association with extension, reducing both the preservation potential of faults and the likelihood that they will be studied.

A crucial requirement of the model is that a wide range of fault lengths is established at an early stage of deformation. One means of departing from conventional models involving initial fault sizes that are small and cover a narrow size range, would be to reactivate pre-existing faults. Areas that are characterised by reactivation of earlier underlying fault systems will inherit something of the characteristics of the older fault system. In the limit, the size distributions of later faults could be the same as those of the underlying established fault system, showing power-law scaling distributions with a large-scale range (Fig. 2). Whatever the precise distribution of size inherited, the new fault system will have the basic property demanded by our model. Within the sequence overlying a reactivated fault system, faults will show a broad range of initial lengths and, at least during the initial stages of fault growth, will have displacements that are under-sized. This model is tested below using a natural dataset.

3. Natural dataset

Using high quality 3-D seismic reflection data, the late Miocene to recent growth history of syn-sedimentary normal faults is established for an area within the Cartier Trough, Timor Sea, Western Australia (Nicol et al., 1996; Meyer et al., 2002). The faults are best imaged within a Tertiary sequence that is dominated by a central graben bounded by two opposed-dipping faults of relatively high maximum displacement (ca. 160 and 170 m) and lengths (ca. 7–8 km) (Fig. 3). These large Tertiary faults form a conjugate structure (for further discussion of conjugate faults refer to Nicol et al. (1995)) and originated by reactivation of Mesozoic normal faults from which they inherited

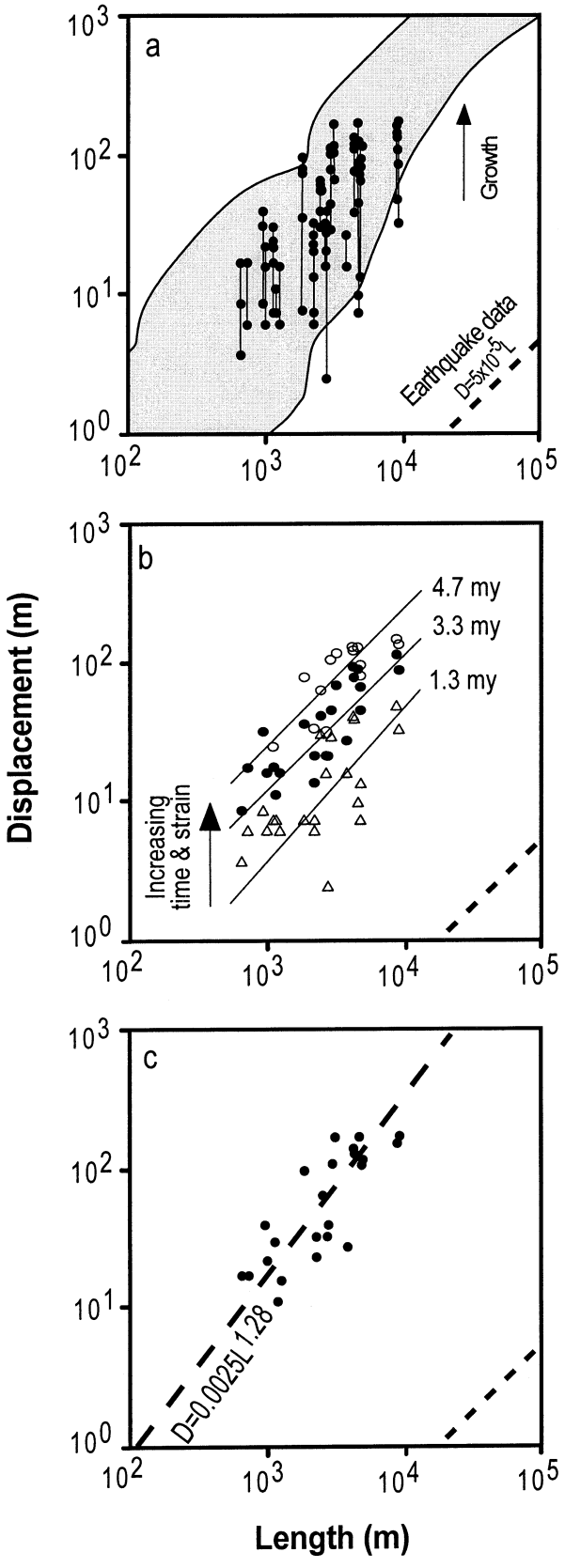

their general strike. Pre-existing Mesozoic structures also partly control the areal distribution of the Tertiary faults, which at the base of the syn-faulting sequence are concentrated within, and NW of, the central graben (Fig. 3). The fault system accommodates about 4.5% extension, with time-averaged extension rates of ca. 0.1 mm/year over the past 6 my (Meyer et al., 2002).

The area is characterised by sedimentation rates that exceed fault displacement rates, a condition that preserves the displacement history of faults as across-fault thickness changes of syn-faulting sedimentary intervals. Up to five syn-faulting sedimentary intervals, each spanning ca. 0.5–1.3 my, blanket much of the fault system. Mapped horizons within the syn-faulting sequence range in age from ca. 6 to 1.3 Ma with progressively younger horizons recording less of the growth history of the system. Meyer et al. (2002) should be referred to for further discussion on the quality of seismic data, measurement of displacements, age determinations of stratigraphy and analysis of faults.

Maximum displacements and lengths can be established at multiple times during the growth of faults by removing displacements on successively older syn-faulting horizons from displacements on the horizon at the base of the syn-faulting sequence, i.e. displacement backstripping (Petersen et al., 1992; Childs et al., 1993). The backstripped maximum displacements and lengths of the 23 largest faults in the area are presented in Figs. 4 and 5. These are the largest 20% of faults in the system at the base of the syn-faulting sequence that have maximum displacements within the map area and trace lengths generally exceeding 1000 m. Fig. 4 shows the growth histories of maximum displacement and length plotted as a function of elapsed time since the onset of faulting. All but one fault nucleated during the first growth interval and their growth curves are assumed to pass through the origin (Fig. 4). Displacement rates for individual faults are, in general, nearly constant with larger faults having higher rates than smaller faults (Nicol et al., 1997; Meyer et al., 2002). The number of active faults gradually decreased over the last ca. 2.5 my with higher mortality rates for those faults with smaller maximum displacement (Meyer et al., 2002). By contrast, the growth in fault lengths was variable through time, with individual faults mainly

Fig. 5. Log–log plots of maximum displacement vs. length for the faults in Fig.4 showing changes in displacement–length relations at the base of the syn-faulting sequence with increasing extension and time from the onset of faulting. (a) Growth paths for individual faults are joined by lines and can be directly compared with the data of Schlische et al. (1996) (shaded region). (b) Data from (a) subdivided according to time at 1.3 my (open triangles), 3.3 my (filled circles) and 4.7 my (open circles) from the onset of deformation. Lines of best fit, produced by double regression, are approximately parallel with slopes of one. (c) Present-day displacements and lengths on faults at the base of the syn-faulting sequence. Equation for the line of best fit is shown. The average position of displacements and lengths of earthquake data from Wells and Coppersmith (1994) are shown on all plots.

attaining their maximum length in the first growth interval (Fig. 4). This initial phase of rapid increase of fault-trace length accounts for no more than ca. 20% of the duration of extension. During the remainder of the period of faulting, trace lengths were either constant or decreased, with continued extension mainly achieved by accumulation of displacements (Meyer et al., 2002; Fig. 4).

Within the resolution of the growth intervals, fault propagation and segment linkage are not important features of this fault system. This is not to say that fault linkage was not important during the first growth interval, as is depicted in Fig. 2b. The lack of linkage may be due in part to the low extension across the fault array with deformation at seismically resolvable relay zones not progressing to the point of breaching. With further extension some of the larger faults in the array may link, as has been widely suggested for other faults (e.g. Peacock and Sanderson, 1991; Childs et al., 1995; Dawers and Anders, 1995; Huggins et al., 1995; Cartwright et al., 1996; McLeod et al., 2000), which would produce a rapid increase in fault length and horizontal growth paths on Figs. 1 and 5a.

The maximum displacement and length characteristics of faults on a horizon that immediately pre-dates faulting record the entire growth history of a fault system. Fig. 5a shows that the faults in the study area have displacement to length ratios that are compatible with previously published data. Maximum displacements and lengths of active faults at different times during faulting (i.e. after 1.3, 3.3 and 4.7 my of extension) show progressively higher displacement to length ratios with time (Fig. 5b). Even at relatively early times, i.e. $\leq$1.3 my after the onset of faulting, the scaling properties of faults are mostly contained within the previously established range for faults (Fig. 5a). Although the displacement–length data in Fig. 5 lies within previously published ranges, the growth of the faults studied is, as predicted by our model, typified by constant lengths and increasing displacement.

The population of active faults has a constant displacement–length slope ($\sim$1.0) through time (Fig. 5b). However, we expect the slope of displacement–length plots for the population containing both the inactive and currently active faults to increase with time and increasing extension (Fig. 5c). This occurs because not all faults are active throughout extension. Instead, progressively more of the smallest faults become inactive while strain is localised onto the larger faults, which continue to accrue displacement but do not increase in length (Figs. 4 and 5a; Meyer et al., 2002). Thus, the existing population of faults comprises smaller faults, which died relatively early and, therefore, have low displacement–length ratios and larger faults, which continue to accrue displacement and have greater displacement–length ratios. Under these circumstances, a plot of displacement against length for the final geometries of all faults will generate a trend with $n > 1$ (e.g. Fig. 5c).

4. Discussion and conclusions

We have developed and tested a model for fault growth in which fault lengths are rapidly established and, thereafter, growth is dominated by accumulating displacement with subdued, if any, lateral propagation of faults. The model predicts that faults within a system will rapidly acquire displacement–length scaling properties that are consistent with previously established fault-growth trends, even though the growth of individual faults differs from those trends.

The cessation of the rapid increase in fault lengths is a key event in the growth history of a fault system, and is attributed to the interaction between fault tips and the consequent retardation in lateral propagation. This process becomes important where the majority of faults in a system begin to interact (e.g. Dawers and Anders, 1995; Cartwright et al., 1996; Nicol et al., 1996; Gupta and Scholz, 2000). High lateral displacement gradients close to tips are generally indicative of fault interaction and are present at ca. 95% of fault tips on the base of the syn-faulting sequence in the Timor Sea dataset (Nicol et al., 1996). The time taken for a fault system to reach these high levels of interaction (e.g. at $>$70% of fault tips) will depend on a number of factors, including, strain rates and the rheology of the crust. In the study area, the largest, but by no means all, faults in the array are reactivated Mesozoic normal faults and account for the initial period of rapid trace lengthening. The presence of earlier faults in the crust quickly localises strain and fault lengths are inherited by up-dip propagation from the underlying structure. Under these circumstances fault lengths can form instantaneously on geological timescales. It is unclear whether this alternative model is applicable to the growth, or some stages in the growth, of fault systems that are not reactivated. Such non-reactivated systems may establish a broad range of initial fault sizes at the earliest stages of faulting and follow the growth model proposed here or as a fault system matures and faults lengthen, it may be characterised by a progressive retardation in fault propagation. There are indications, for example, that the later stages of growth of normal-fault systems in the Aegean are characterised by limited fault propagation and a progressive increase in the ratio of displacement to length for individual faults with time (Armigo et al., 1996; Morewood and Roberts, 1999; Poulimenos, 2000). In addition, the observations of Morley (1999) in the East African Rift suggest that throughout the evolution of the rift, basin bounding faults show no clear evidence of lateral propagation, while Childs et al. (2002) also document limited propagation of faults in the North Sea. It is clear therefore, that for some fault systems the ratio of displacement to length is not constant through time, and that a progressive increase in displacement–length ratio could reflect fault system maturity. Future work should be directed towards the kinematic analysis of faults because discrimination between the

two types of fault-growth model is not possible using geometric constraints alone.

Acknowledgements

This paper is the result of studies completed in the Fault Analysis Group at the University of Liverpool and University College Dublin with financial support from the Royal Society of New Zealand Marsden Fund (Grant number GNS 902) and EU 4th Framework Grant (JOF3-CT97-0036). We thank other members of the Fault Analysis Group, in particular Juan Watterson and Tom Manzocchi, for discussions on fault-related growth issues. N. Dawers and Z. Shipton provided constructive reviews of the manuscript.

References

Armigo, R., Meyer, B., King, G.C.P., Rigo, A., Papanastassiou, D., 1996. Quaternary evolution of the Corinth Rift and its implications for the Late Cenozoic evolution of the Aegean. Geophysical Journal International 126, 11–53.

Cartwright, J.A., Mansfield, C., Trudgill, B., 1996. The growth of faults by segment linkage. In: Buchanan, P.G., Nieuwland, D.A. (Eds.), Modern Developments in Structural Interpretation, Validation and Modelling. London Geological Society, Special Publication 99, pp. 163–177.

Childs, C., Easton, S.J., Vendeville, B.C., Jackson, M.P.A., Lin, S.T., Walsh, J.J., Watterson, J., 1993. Kinematic analysis of faults in a physical model of growth faulting above a viscous salt analogue. Tectonophysics 228, 313–329.

Childs, C., Watterson, J., Walsh, J.J., 1995. Fault overlap zones within developing normal fault systems. Journal of the Geological Society 152, 535–549.

Childs, C., Nicol, A., Walsh, J.J., Watterson, J., 2002. The growth and propagation of syn-sedimentary faults. Journal of Structural Geology in press.

Cowie, P.A., Scholz, C.H., 1992. Physical explanation for displacement–length, relationship for faults using a post-yield fracture mechanics model. Journal of Structural Geology 14, 1133–1148.

Cowie, P.A., Shipton, Z.K. 1998. Fault tip displacement gradients and process zone dimensions. Journal of Structural Geology 20, 938–997.

Dawers, N.H., Anders, M.H. 1995. Displacement–length scaling and fault linkage. Journal of Structural Geology 17, 607–614.

Dawers, N.H., Anders, M.H., Scholz, C.H., 1993. Fault length and displacement: scaling laws. Geology 21, 1107–1110.

Gillespie, P.A., Walsh, J.J., Watterson, J., 1992. Limitations of dimension and displacement data from single faults and the consequences for data analysis and interpretation. Journal of Structural Geology 14, 1157–1172.

Gupta, A., Scholz, C.H., 2000. A model of normal fault interaction based on observations and theory. Journal of Structural Geology 22, 865–879.

Huggins, P., Watterson, J., Walsh, J.J., Childs, C., 1995. Relay zone geometry and displacement transfer between normal faults recorded in coal-mine plans. Journal of Structural Geology 17, 1741–1755.

McLeod, A.E., Dawers, N.H., Underhill, J.R., 2000. The propagation and linkage of normal faults: insights from the Strathspey–Brent–Statfjord fault array, northern North Sea. Basin Research 12, 263–284.

Meyer, V., Nicol, A., Childs, C., Walsh, J.J., Watterson, J., 2002. Progressive localisation of strain during the evolution of a normal fault system in the Timor Sea. Journal of Structural Geology 24, 1215–1231.

Morley, C.K., 1999. Patterns of displacement along large normal faults: implications for basin evolution and fault propagation, based on examples from East Africa. Bulletin of the American Association of Petroleum Geologists 83, 613–634.

Morewood, N.C., Roberts, G.P., 1999. Lateral propagation of the surface trace of the South Alkyonides normal fault segment, central Greece: its impact on models of fault growth and displacement–length relationships. Journal of Structural Geology 21, 635–652.

Nicol, A., Walsh, J.J., Watterson, J., Bretan, P., 1995. The three-dimensional geometry and growth of conjugate normal faults. Journal of Structural Geology 17, 847–862.

Nicol, A., Walsh, J.J., Watterson, J., Childs, C., 1996. The shapes, major axis orientations and displacement patterns of fault surfaces. Journal of Structural Geology 18, 235–248.

Nicol, A., Walsh, J.J., Watterson, J., Underhill, J.R., 1997. Displacement rates of normal faults. Nature 390, 157–159.

Peacock, D.C.P., Sanderson, D.J., 1991. Displacements, segment linkage and relay ramps in normal fault zones. Journal of Structural Geology 13, 721–733.

Petersen, K., Clausen, O.R., Korstgård, J.A., 1992. Evolution of a salt-related listric growth fault near the D-1 well, block 5605, Danish North Sea: displacement history and salt kinematics. Journal of Structural Geology 14, 565–577.

Poulimenos, G., 2000. Scaling properties of normal fault populations in the western Corinth Graben, Greece: implications for fault growth in large strain settings. Journal of Structural Geology 22, 307–322.

Schlische, R.W., Young, S.S., Ackermann, R.V., Gupta, A., 1996. Geometry and scaling relations of a population of very small rift-related normal faults. Geology 24, 683–686.

Scholz, C.H., 1982. Scaling laws for large earthquakes: consequences of physical models. Bulletin of the Seismological Society of America 72, 1–14.

Scholz, C.H., Cowie, P.A., 1990. Determination of total strain from faulting using slip-measurements. Nature 346, 837–839.

Walsh, J.J., Watterson, J., 1988. Analysis of the relationship between the displacements and dimensions of faults. Journal of Structural Geology 10, 239–247.

Wells, D.L., Coppersmith, K.J., 1994. New empirical relationships among magnitude, rupture length, rupture width, rupture area, and surface displacement. Bulletin of the Seismological Society of America 84, 974–1002.